JOURNAL OF GEOPHYSICAL RESEARCH, VOL. 95, NO. D13, PAGES 22,547–22,557, DECEMBER 20, 1990

Atmospheric Response to Ice Age Conditions: Climatology Near the Earth's Surface

M. LAUTENSCHLAGER AND K. HERTERICH

Max-Planck-Institut für Meteorologie, Hamburg, Federal Republic of Germany

We present a 6-year simulation of the ice age atmosphere using the T21 Atmospheric General Circulation Model (AGCM) of the European Centre for Medium-Range Weather Forecasts (ECMWF). The lower boundary conditions (18 kyr B.P.) were taken from CLIMAP Project Members (1981). The analysis is restricted to the surface climatology for two reasons: The surface fields are the test data derived from the geological record on land, and they define the upper boundary conditions for simulating the glacial ocean. Model results are shown for the mean annual surface fields of temperature, wind, and precipitation. In the global average the surface temperature was 4.7°C cooler compared to the present temperature. The wind strength increased in mid-latitudes and decreased in tropical trade wind regions. Precipitation did not change significantly in the global average; however, precipitation decreased over land and increased over the ocean. Most of the difference patterns between the present conditions and the ice age climate were statistically significant. The simulated surface climatology is roughly consistent with the paleogeological evidence and with numerical AGCM simulations of other authors. This suggests that presently available AGCMs, including the ECMWF model (T21), are able to describe climates far away from the present, although internal parameterizations were tuned to present data sets.

1. INTRODUCTION

During the last 20 years, a growing volume of data has been collected on past climates, derived from the analysis of terrestrial and ocean sediments and ice cores. These data cover a wide range of variables describing atmosphere, ocean, ice, and biosphere, the components of the climate system. The data set is especially dense at the time of the last glacial maximum, 18,000 years before present (18 kyr B.P.). For this period a complete data set is now available, enabling the prescription of the boundary conditions for an Atmospheric General Circulation Model (AGCM) (sea surface temperature, distribution of land and sea ice, and land albedo) and providing test data on atmospheric conditions, such as surface temperature and surface humidity on land, and wind data at some locations. Thus the ice age climate 18 kyr B.P. represents a unique opportunity to test an AGCM. If the simulation is successful, it will yield a much more detailed reconstruction of the atmospheric state in the past than could be extracted only from the geological record. The modeled atmospheric state may be applied then to simulate the ice age ocean, using boundary conditions partly calculated from the AGCM.

Most AGCMs were designed with model parameterizations tuned to give a good representation of the present atmospheric state. Because of model deficiencies and limited resolution it is not obvious that these models will also yield a realistic simulation under widely changed climatic conditions, such as the last glacial maximum or for a doubled atmospheric carbon dioxide concentration. A comparison of numerical experiments with different AGCMs using the same boundary conditions is therefore needed to sort out model deficiencies and to assess the ability of AGCMs to predict climatic change.

AGCM simulations of the last glacial maximum 18 kyr B.P. including the annual cycle, have been performed by *Broccoli and Manabe* [1987], *Manabe and Broccoli* [1985*a*, *b*], and *Rind* [1987] and simulations excluding the annual cycle by *Gates* [1976] and *Kutzbach and Guetter* [1986]. To some extent the numerical experiments presented below repeat these experiments, but the inclusion of a hypothetical Tibetan ice sheet, the use of a different AGCM (the T21 model of the European Centre for Medium-Range Weather Forecasts (ECMWF)), and the evaluation of the statistical significance of the results (*t* test, *F* test, pattern correlation) contribute new aspects. The model results in the tropics and in Antarctica, two critical regions in AGCM simulations, will be considered in more detail. Results will be shown for the annual means of the following three near-surface variables: temperature at 2-m height, wind at 10-m height, and precipitation. The glacial surface climatology is presented in a way which allows for direct comparison to the geological data.

In section 2, a short description of the model is presented, and the ice age boundary conditions are specified. Section 3 summarizes the model results, including the statistical significance tests. A comparison of the model results with observations and with other simulations follows in sections 4 and 5, respectively. Our main conclusions are outlined in section 6.

2. MODEL AND EXPERIMENT

2.1. *Model Components*

The AGCM used is the T21 model developed at the ECMWF as described by *Louis* [1984] and modified by *Dümenil and Schlese* [1987] for climate simulations. The T21 AGCM is based on the primitive equations with radiation, a hydrological cycle including predicted clouds, and a three-layer soil model, determining soil temperature and soil moisture. The model equations are solved in the spectral domain and truncated at wave number 21 (triangular truncation). This corresponds to a horizontal resolution of 5.6° in latitude and longitude. The vertical coordinate is resolved by 16 levels in a hybrid coordinate system; the terrain-following

Paper number 90JD02064.
0148-0227/90/90JD-02064$05.00

TABLE 1. Orbital Parameters

	Eccentricity	Obliquity, deg	Perihelion, deg
Present	0.0167	23.45	282
18 kyr B.P.	0.0195	23.44	344

sigma coordinate at low model levels is transformed to pressure coordinates at higher levels, yielding surfaces of constant pressure in the stratosphere.

2.2. *Model Performance*

A comparison of the modeled present-day temperature and wind fields near the Earth's surface with corresponding 850-hPa data from the ECMWF climatology, based on daily analyses from 1981 to 1985, shows that the T21 model is able to simulate the present climate, although not perfectly. At the poles the model is 2°–3°C too warm, while at the equator it is too cold by about the same amount. The meridional temperature gradient is therefore underestimated, and the resulting winds are 20% too weak on average. Locally, larger errors occur. The largest errors occur for the westerlies around 50°S, which have only 50% of the observed strength. The general structure of global wind patterns, however, is simulated quite realistically. The monthly means of precipitation were compared with the corresponding climatology published by *Jaeger* [1976]. Again, the global patterns of precipitation are simulated quite realistically, except in the tropics, where the precipitation maxima are underestimated by up to 50%.

2.3. *Ice Age Boundary Conditions*

For the AGCM ice age experiment the following model input parameters and boundary conditions were changed from modern to ice age conditions (18 kyr B.P.): Orbital parameters, atmospheric CO_2 concentration, coastlines, orography, sea surface temperature, surface albedo on land, and deep soil temperature and moisture.

Orbital parameters. The elliptical orbit of the Earth around the Sun is characterized by three parameters: eccentricity, obliquity (the angle between the Earth's axis and the normal to the ecliptic), and longitude of perihelion (the angle between the vernal equinox (beginning of springtime) and perihelion (time of nearest distance to the Sun), measured counterclockwise from vernal equinox). The values for 18 kyr B.P. were taken from *Berger* [1978]. They are listed in Table 1 together with the present day values.

The orbit of the Earth was somewhat more elliptical 18 kyr B.P. than today, while the obliquity practically did not change. Today, perihelion lies around January 1, compared to March 15, 18 kyr B.P. These rather small changes in the orbital parameters reduced July insolation at 65°N at glacial maximum by about 1%.

CO_2 concentration. The atmospheric CO_2 concentration, which is presently 330 ppm (1975), was set to 200 ppm in the ice age experiment, in accordance with CO_2 measurements from the Vostok ice core [*Barnola et al.*, 1987].

Coastlines. Coastlines were changed at the last glacial maximum (mainly in coastal shelf areas) by assuming a sea level reduction of 100 m.

Orography. The elevation of the ice age sheets was taken from *CLIMAP Project Members* [1981]. In addition, a glaciation of the Tibetan highlands after *Kuhle* [1987] was added. The existence of a Tibetan ice sheet at the last glacial maximum is still disputed. In a sensitivity experiment using the T21 AGCM a significant global atmospheric response to a hypothetical Tibetan ice sheet was not found [*Lautenschlager and Santer*, 1990]. Apart from local effects, such as a reduction of the glacial Indian summer monsoon, the ice age experiment performed with the T21 model can therefore be directly compared with AGCM experiments of other authors without assuming a glacial Tibetan ice sheet.

Sea surface temperature. The sea surface temperature (SST) was taken from *CLIMAP Project Members* [1981] for February and August. The annual cycle of SSTs was approximated by a cosine function, taking the values for February and August as extrema.

Surface albedo. The model surface albedo used was 0.6 for land ice and snow and 0.55 for sea ice. The ocean surface albedo was set at 0.07. The same values were chosen for the control run with modern boundary conditions. The surface albedo of land points free from ice and snow was taken from *CLIMAP Project Members* [1981]. Ten albedo classes between 0.1 and 0.5 were specified in the model.

Deep-soil temperature and moisture. The surface temperature and moisture at land points are calculated in the T21 model by a three-layer soil model. At the lower boundary, at soil depth 70 cm, monthly mean moisture and temperature have to be specified. As the deep-soil boundary conditions cannot be obtained from geological data at the last ice age maximum, they are specified according to the following consideration: The largest changes in the soil conditions are expected to occur at the locations of the ice age ice sheets. Therefore the deep-soil boundary conditions in the ice age experiment were changed only at the positions of the ice age ice sheets, taking the values used for the Greenland ice sheet in the control run. The dependence of the global climatic response on the deep-soil boundary conditions is expected to be weak (2/3 of the Earth's surface is covered with water), but their regional influence is probably not negligible. In a sensitivity experiment (permanent ice age January conditions) the deep-soil temperature was globally reduced by 10°C. Nevertheless, the global AGCM response was comparable to the atmospheric ice age simulation presented except for some unrealistic regional features (surface temperatures in January below freezing in the Sahara).

2.4. *Statistical Significance*

Two AGCM experiments, an ice age run and a present-day control run, were performed. For both experiments, six annual cycles were calculated. After 1 year for model spin-up the last five model years were used to compute the climatic averages. The significance of the atmospheric ice age response was estimated by comparing the means, the variances and spatial patterns for both, the control and ice-age run.

The comparison of the means was performed in terms of univariate t statistics. At each grid point the hypothesis of different monthly means was tested at the 99% confidence level. The univariate F statistic was applied to the comparison of variances in time. At each grid point the hypothesis of different interannual variability was tested at the 99% confidence level. The comparison of spatial patterns for the

TABLE 2. Global Average of Annual Mean Temperature at 2-m Height

	All Points	Land Points	Ocean Points
Ice Age Experiment			
Mean	9.2	2.5	12.7
Interannual variability	0.8	1.2	0.5
Amplitude of annual cycle	5.3	10.1	2.7
Present-Day Control Experiment			
Mean	13.9	9.5	15.6
Interannual variability	0.7	1.2	0.4
Amplitude of annual cycle	4.7	10.3	2.5

Units are degrees Celsius.

time-mean fields was expressed by a spatial correlation coefficient. (For detailed information on the statistical calculations, see *Wigley and Santer* [1990] and *Santer and Wigley* [1990]). The results of the univariate statistical analysis appeared sufficiently convincing that it did not seem to be necessary to apply more elaborate multivariate statistics.

3. Model Results

In the following, results will be shown for the annual means only, although the 6-year simulation of the ice age atmosphere and the control run were performed by including the seasonal cycle.

3.1. *Global Means*

The globally averaged results of the experiments are summarized in Table 2 for the temperature at 2-m height and in Table 3 for precipitation. Comparison of the ice age experiment with the present-day control run shows that the interannual variability and the amplitude of the annual cycle were similar in both experiments. The global mean temperature was 4.7°C lower at glacial maximum, but the global mean precipitation did not change significantly. For better comparison with data, these global averages were split into land points (including the ice sheets) and ocean points (including sea ice). The glacial response of the land surface was stronger than the response of the ocean.

On land, surface temperatures were reduced by 7.0°C, and precipitation was decreased by 0.26 mm/d (13%). The amplitude of the annual cycle decreased by 17% for precipitation.

Over the ocean, surface temperature decreased by 2.9°C, and precipitation increased slightly by 0.11 mm/d (5%). The oceanic response was dictated by the prescribed SSTs and by the larger glacial temperature contrast between land and ocean. Stronger glacial bursts of cold continental air increased evaporation regionally. The cold air could not hold the additional moisture content, resulting in a regionally increased precipitation. This mechanism was also reflected by the surface heat fluxes. The decreased precipitation over land and the increased precipitation over the ocean compensated each other in the model, yielding practically no change in the glacial precipitation in the global and annual average.

3.2. *Zonal Means*

The meridional structure of the glacial surface climatology as simulated by the T21 model is presented in Figures 1, 2, and 3. The anomalies (ice age experiment minus present-day control run), also separated into land points and ocean points, are given in dimensional units and as percentage change of the present-day values for better comparison with geological data.

The glacial reduction of the near-surface temperature (Figure 1*a*) increases from the equator (2°C) to the poles (north pole 13°C, south pole 14°C). At tropical land surfaces between 20°N and 20°S the temperature decreased in the range 2°–4°C (Figure 1*b*).

The zonally averaged glacial wind strength, defined as the absolute value of the monthly mean wind vector, is presented in Figures 2*a*–2*c*. At the ice sheet locations (50°–80°N), the near-surface circulation strongly increased over both the ocean and land. The southern hemisphere westerlies (40°–50°S) increased by 70%. In the subtropics the wind strength increased up to 50% over the ocean. The glacial surface winds in the tropics (20°N–20°S), however, were reduced up to 40% over the ocean and 30% over land.

Figure 3 shows the zonally averaged glacial precipitation. The pronounced precipitation increase over the oceans in the subtropics and in the mid-latitudes is consistent with a stronger glacial circulation in these areas. At land surfaces the glacial precipitation was generally reduced compared to the present.

3.3. *Global Fields*

In Figure 4 the global pattern of the atmospheric temperature response is shown. Temperatures were reduced up to 5°C in the tropical land areas and were approximately 20°C cooler in the glaciated areas (Figure 4*c*).

The most pronounced change in the wind field from present to glacial conditions occurred near the ice age ice sheets of the northern hemisphere and the Antarctic ice sheet. Part of the westerlies of the northern hemisphere follows a branch along the northern edge of the ice sheets, which is missing in the control run (Figure 5). The trade winds did not alter in the Atlantic sector, while the Pacific trade winds west of Peru significantly decreased (Figure 5*c*).

The response in precipitation has a complicated structure (Figure 6). Nevertheless, an overall reduction in precipitation in the ice age experiment (Figure 6*c*) is visible in tropical land areas and over the ice sheets (North America, northern Europe, Siberia, and Tibet). The precipitation in India decreases (Figure 6*c*) due to a reduction of the summer monsoon circulation at the last glacial maximum [*Duplessy*, 1982]. This response cannot be uniquely related to the

TABLE 3. Global Average of Annual Mean Precipitation

	All Points	Land Points	Ocean Points
Ice Age Experiment			
Mean	2.27	1.76	2.55
Interannual variability	0.84	0.70	0.91
Amplitude of annual cycle	0.99	1.00	0.98
Present-Day Control Experiment			
Mean	2.32	2.02	2.44
Interannual variability	0.81	0.79	0.81
Amplitude of annual cycle	1.03	1.20	0.96

Units are millimeters per day.

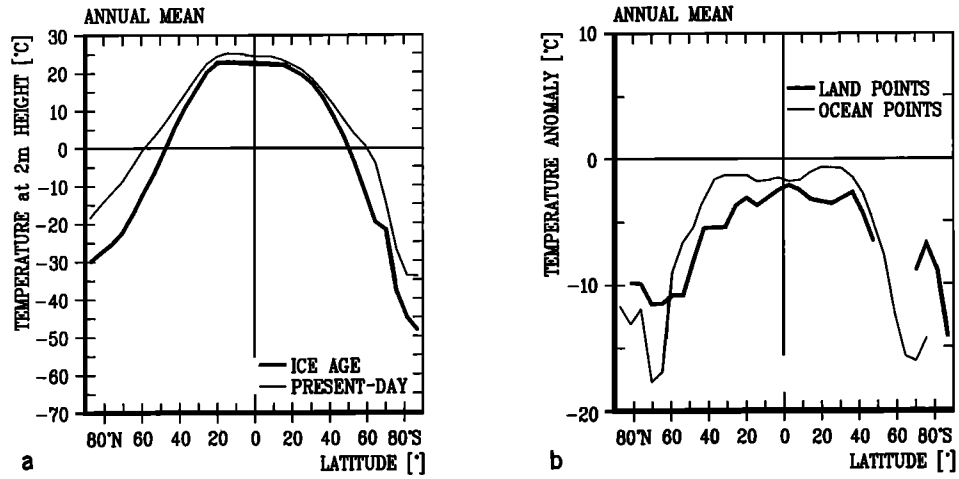

Fig. 1. Zonal averages of (*a*) annual mean temperature at 2-m height and (*b*) anomaly (ice age minus present) of 2-m height temperature.

existence of a Tibetan ice sheet in the ice age experiment [*Lautenschlager and Santer*, 1990].

3.4. *Significance*

The significance was evaluated by univariate t statistics for the monthly means and in terms of the univariate F statistics for the interannual variability. The modification of spatial patterns in the time-mean fields was expressed by a spatial pattern correlation coefficient which is a measure for similarities in the basic global structure of the selected atmospheric quantities. The averages of the statistical tests for January, April, July, and October are summarized in Table 4. In columns 2 and 3 the percentage of grid points is listed, for which the hypothesis of different monthly means and different interannual variability, respectively, is accepted at a confidence level of 99%. Column 4 contains the pattern correlation coefficients.

As can be inferred from the global averages in Tables 2–4, the modeled mean ice age climate is significantly different from the present-day climate. The interannual variability and the amplitude of the annual cycle (simulated with prescribed climatological ocean) were not significantly different between ice age and present-day conditions. Both climate states, present and 18 kyr B.P., are characterized by similar spatial patterns in the time-mean fields.

4. Comparison of Model Results With Observations

Recently, *Crowley* [1988] and *Crowley and North* [1989] summarized data on the 18 kyr B.P. climate which has been reconstructed from the geological record. In particular, *Crowley* [1988] compares model results with geological data and concludes that the response of AGCMs to ice age boundary conditions generally agrees with data in mid-latitudes of the northern hemisphere. In tropical regions and in Antarctica, however, there still are significant differences between models and data and between the models themselves. These areas will be considered in more detail below.

4.1. *Temperature*

The glacial surface temperature on land decreased in the range 5°–10°C for a large number of areas [*Crowley and*

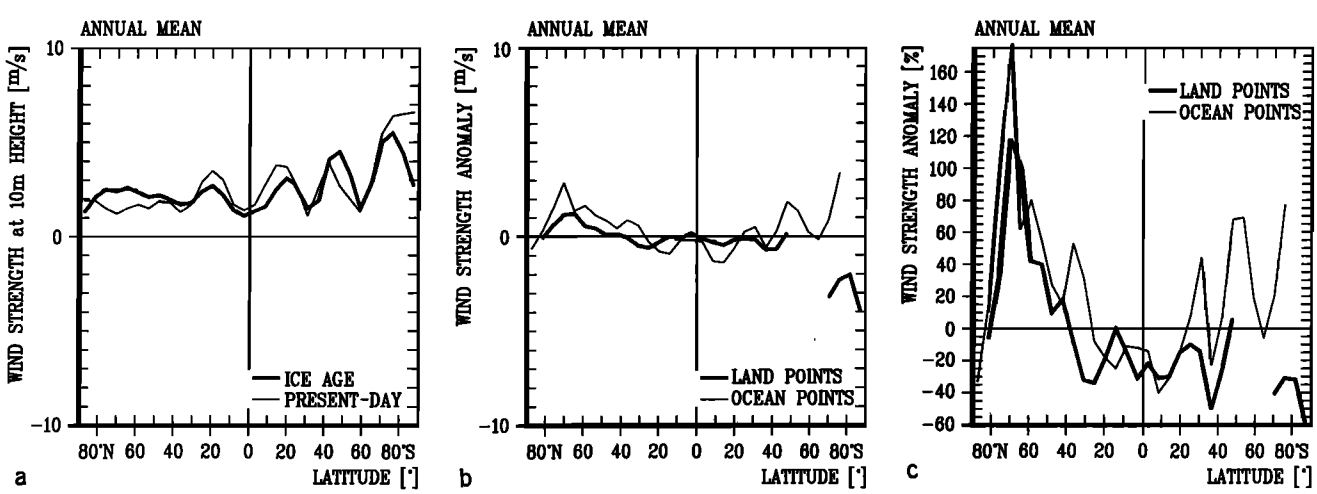

Fig. 2. Zonal averages of (*a*) annual mean wind strength at 10-m height, (*b*) anomaly (ice age minus present) of 10-m wind strength, and (*c*) change of present-day wind strength.

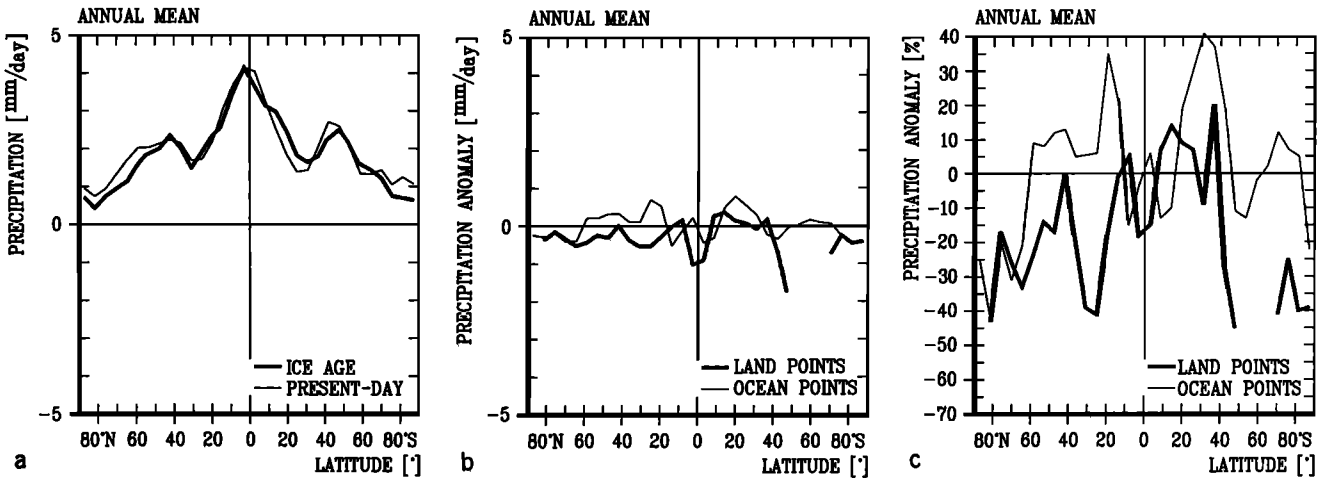

Fig. 3. Zonal averages of (*a*) annual mean precipitation, (*b*) anomaly (ice age minus present) of precipitation, and (*c*) change of present-day precipitation.

North, 1990]. In the global average the model reduced land temperatures by 7°C (see Table 2). In East Antarctica a glacial temperature decrease of 8°–9°C is derived from the Vostok ice core [*Jouzel et al.*, 1987]. This Antarctic temperature decrease was simulated by the T21 model (compare Figures 1 and 4).

In the tropical land areas the glacial temperature reduction is disputed. *Liu and Colinvaux* [1985] claim a temperature decrease of 4°–6°C in the lowlands of the western Amazon Basin, but their data were evaluated at a site elevation of 1100 m. *Crowley* [1988] argues for a smaller temperature decrease (around 2°C) in the tropical lowlands because of the small reduction in glacial SSTs. In the model the zonally averaged land temperature decreased by 2°–4°C between 20°N and 20°S (Figure 1*b*). In particular, the lowland temperature was reduced by 0.5°–2.5°C for the Amazon Basin and 1.0°–2.5°C for the Congo Basin.

Rind and Peteet [1985] evaluated geological data of the glacial snow line depression in the tropics. They calculate a snow line lowering of 950 m and a corresponding temperature depression in high altitudes of 8°–10°C for the Colombian Andes (elevation 4000–6000 m). For the African sites, Mount Kilimanjaro (elevation 5963 m) and Mount Kenya (elevation 5194 m), the glacial snow line was lowered by 900 m, and the high-altitude temperature decreased by more than 4.5°C. *Messerli* [1980] obtains similar results for the African tropical mountains. The T21 model yielded a glacial temperature reduction of 4.0°C for the Colombian Andes and 3.3°C for the African mountains, which is smaller than the observed values but considerably larger than the lowland temperature reduction. The averaged model grid point elevations of 3000 m for the Andes and 1000 m for the African sites are lower than the glacial equilibrium line of glaciation. Therefore the model simulated no permanent snow coverage, and an additional temperature decrease due to the ice-albedo feedback was not included.

4.2. *Wind*

The T21 model produced a splitting of the ice age jet stream over the Laurentide ice sheet in the higher atmospheric wind fields. The surface wind increased strongly north of this ice sheet (Figures 2 and 5*c*). In the northern hemisphere mid-latitudes the wind strength increased in the range 20–80% (Figure 2*c*). A southwesterly flow in Alaska resulted in generally mild ice age climates [*Crowley*, 1988]. The T21 model, however, did not simulate an intensification of the southwesterly flow in Alaska (Figure 5*c*). Strong northwesterly winds in the channel between the Laurentide and Greenland ice sheet (Figure 5*c*) advected very cold air into the northwestern Atlantic which may have caused the observed equatorward displacement of sea ice. In Europe, advection of cold air combined with local cooling due to the Eurasian ice sheet resulted in winter temperature anomalies 20°–25°C [*Crowley*, 1988] which are larger than for any other land area (compare Figure 4*c*).

At the last glacial maximum, *Petit et al.* [1981] observe a pronounced dust increase in the East Antarctic ice cores and infer an increase of wind strength in the Subantarctic region of 50–80%. In the ice age experiment the zonally averaged wind strength over the ocean around Antarctica increased by 70% at 50°S (Figure 2*c*).

The frequently cited glacial response in the tropical trade wind region is an increase in wind strength of 30–50% [*Crowley and North*, 1990]. This number is based on the observed increase of atmospheric dust content and on the intensification of near-coastal upwelling as derived from tropical marine sediment cores. In contrast, the T21 model showed a glacial reduction of the zonally averaged tropical wind strength over the ocean of 10–15% (Figure 2*c*) and up to 50% in the tropical Pacific. The latter model result, however, is supported by a marine sediment core from the central tropical Pacific [*Pisias and Rea*, 1988]. In this core the grain size of eolian dust has a sharp minimum for the last glacial maximum. The grain size is a better indicator of the mean wind strength, which is responsible for the long-range transport, than the atmospheric dust content itself. The dust content is more correlated to the aridity and to the wind fluctuations on short-time scales. These model results are also consistent with first-order arguments. The trade wind intensity should be related to the strength of the Hadley circulation. At the last glacial maximum the meridional SST gradient decreased in the tropics of the Pacific (tropical

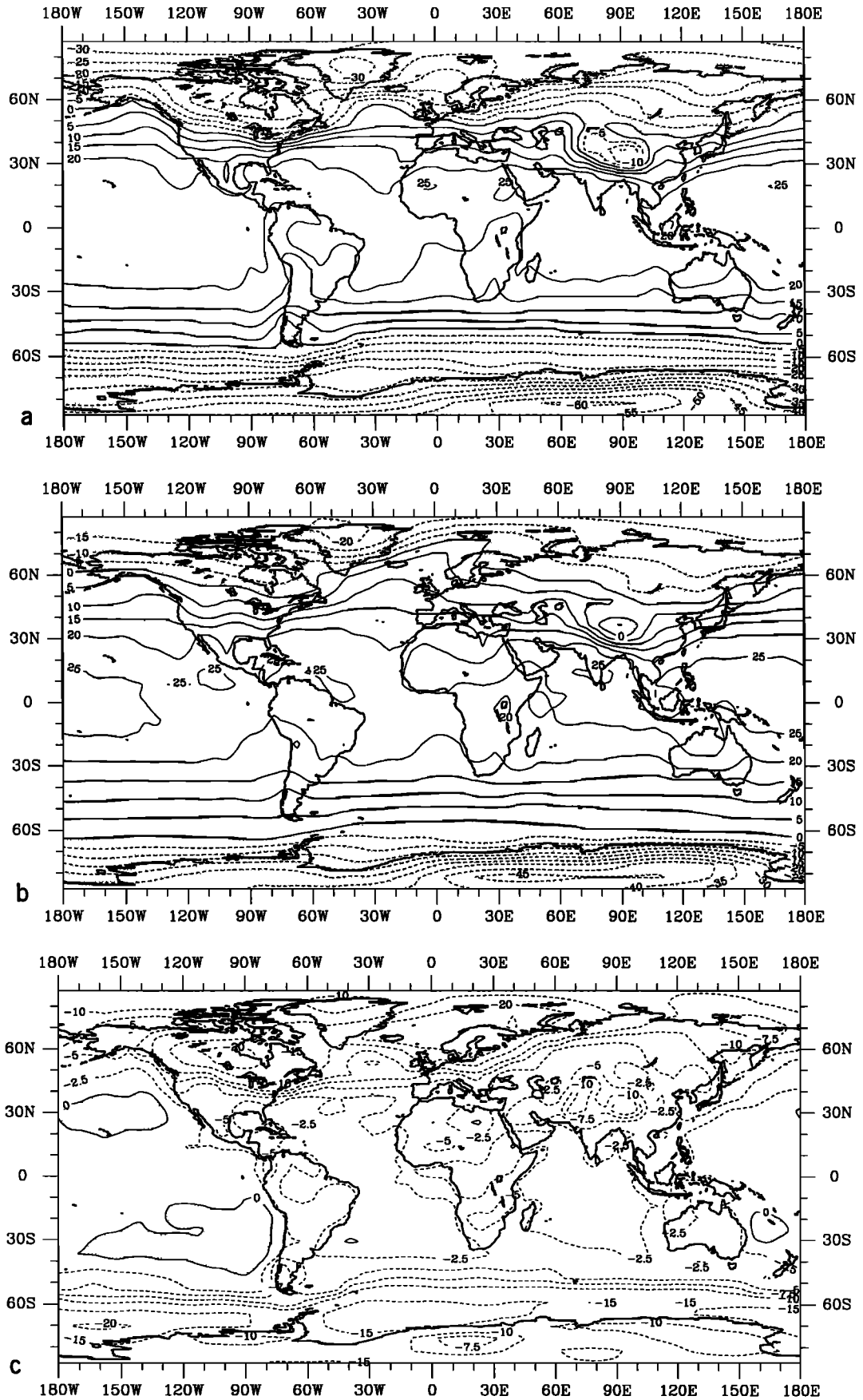

Fig. 4. Annual mean temperature at 2-m height: (*a*) ice age experiment, (*b*) present-day control experiment, and (*c*) anomaly (ice age minus control run). Units are degrees Celsius.

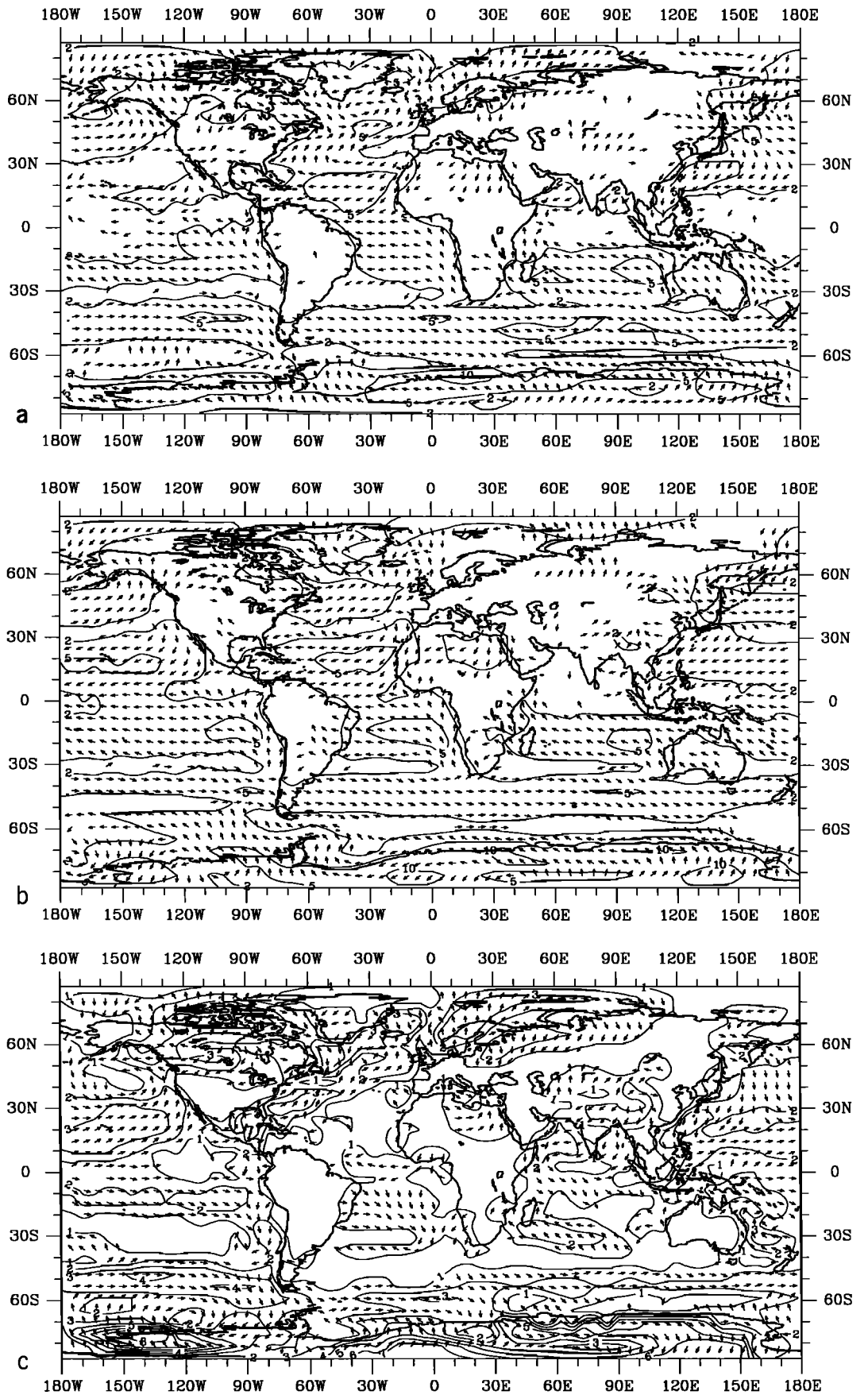

Fig. 5. Annual mean wind at 10-m height: (*a*) ice age experiment, (*b*) present-day control experiment, and (*c*) anomaly (ice age minus control run). (Vectors less than 1 m/s are omitted.) Units are meters per second.

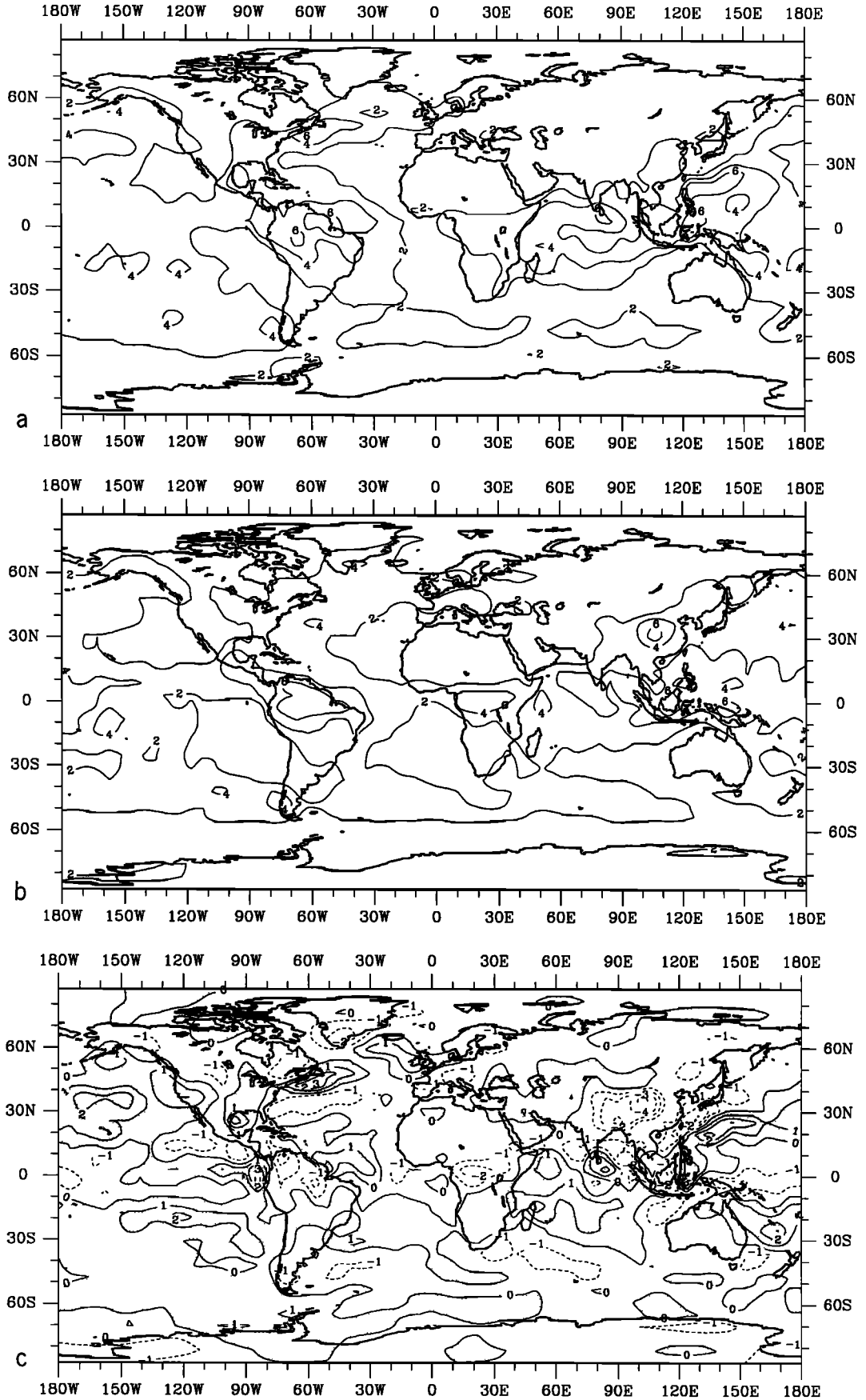

Fig. 6. Annual mean precipitation: (*a*) ice age experiment, (*b*) present-day control experiment, and (*c*) anomaly (ice age minus control run). Units are millimeters per day.

TABLE 4. Annual Average Statistics

	Mean, % of points	Interannual Variability, % of points	Pattern Correlation
Temperature at 2 m	90	2	0.98
Zonal wind at 10 m	26	2	0.76
Meridional wind at 10 m	27	2	0.63
Precipitation	16	5	0.73

Confidence level is 99%.

cooling and subtropical warming, compare Figure 4c). Thus the Pacific Hadley circulation and the trades should be reduced in the model.

Provided the model results are correct, the observed stronger coastal upwelling in the tropical Pacific, as reported by *Sarnthein et al.* [1988], has to be explained by mechanisms other than intensified trade winds. These mechanisms include changes in the oceanic circulation and/or in mesoscale atmospheric wind patterns not resolved in the T21 model. A preliminary, yet unpublished attempt to simulate the glacial ocean circulation with the Hamburg Large Scale Geostrophic Ocean Model shows deepwater production in the North Pacific. If this is balanced by the production of Antarctic bottom water, it might result in an increased equatorial upwelling. There are also indications that easterly winds were stronger in the near-coastal area due to stronger downslope winds from the Andes. The land-sea temperature contrast was larger at glacial maximum compared to the present. This is visible in both the data [*Rind and Peteet*, 1985] and in the T21 model. On the basis of the shallow water theory [*Atkinson*, 1981] the glacial intensification of downslope winds from the Andes may be estimated to a factor of 4–6.

4.3. *Precipitation*

In the global average the model precipitation decreased by 13% over land. This was roughly compensated by an increase of precipitation over the ocean. As has been inferred from geological data, the acceleration of the flow in the jet entrance region of the United States led to relatively low-pressure systems with increased precipitation in the southwest which is supported by high glacial lake levels in this region [*Crowley*, 1988]. In the T21 model the glacial precipitation increased more in the west than in the southwest.

The glacial reduction of tropical rain forests to several refugia in regions of highest modern rainfall [*Messerli*, 1980; *Liu and Colinvaux*, 1985] might be explained by a reduction of tropical precipitation. On the other hand, *Street-Perrott and Harrison* [1984] find that the tropical lake levels did not change at 18 kyr B.P. At the last glacial maximum the tropics seemed to be as arid as today, and therefore only minor changes in the freshwater balance (precipitation minus evaporation) can be expected. According to the Clausius-Clapeyron equation a tropical lowland temperature reduction of 2°C results in an evaporation decrease of 20–30%. The tropical precipitation reduction should then be of the same order of magnitude if no change in the freshwater balance is to be expected. The tropical precipitation reduction, as simulated by the T21 model, fits into this picture (Figure 3c): The precipitation is reduced by 12% in the Amazon Basin and 20% in the Congo Basin.

5. COMPARISON WITH OTHER AGCMS

Comparison with simulations of other authors is restricted here to simulations of the last glacial maximum which are comparable with respect to the specified boundary conditions.

5.1. *Geophysical Fluid Dynamics Laboratory Model*

A variety of experiments simulating the last glacial maximum [*Broccoli and Manabe*, 1987; *Manabe and Broccoli*, 1985*a*, *b*] was performed by using a spectral climate model developed at the Geophysical Fluid Dynamics Laboratory (GFDL) of NOAA. The spectral domain is truncated rhombically at wave number 15, which yields a horizontal spatial resolution comparable to the T21 AGCM. The vertical resolution is nine levels. The GFDL model is comparable to the T21 model with regard to model physics. The global atmosphere was coupled to a mixed-layer ocean. Therefore the SST is a predicted quantity in the GFDL model and has not needed to be prescribed, as in other AGCMs. The mixed-layer ocean takes into account the heat storage capacity of the ocean but neglects the glacial changes in the oceanic heat transport. In the global average a glacial SST reduction of 1.9°C was simulated [*Broccoli and Manabe*, 1987] which is comparable to the *CLIMAP Project Members* [1981] value of 1.6°C. However, the regional distribution of simulated SST is different from the CLIMAP maps [*Manabe and Broccoli*, 1985*b*]. This might be the most probable reason for differences in the atmospheric response at 18 kyr B.P. between the GFDL model and other AGCMs.

Manabe and Broccoli [1985*a*] performed an ice age simulation including cloud radiation feedback, also contained in the T21 model. The global reduction of annual mean surface air temperature is 4.7°C, which is exactly the T21 result. The zonally averaged reduction of surface air temperature over land and over the ocean is comparable to the T21 results, except Antarctica, where the T21 AGCM simulated a stronger temperature reduction. *Manabe and Broccoli* [1985*b*] examine the influence of continental ice. This experiment is only roughly comparable to the T21 ice age run because the albedo on land, free from ice and snow, and the atmospheric CO_2 concentration were fixed to modern values. Nevertheless, the cooling patterns over land of the GFDL model and the T21 AGCM have a similar structure. The cooling over the Eurasian ice sheet and over Antarctica is stronger in the T21 experiment. The GFDL model even simulated glacial warming in small regions of Antarctica.

The GFDL surface wind patterns for the northern hemispheric winter season [*Manabe and Broccoli*, 1985*b*] are also comparable with the T21 simulation. A jet stream splitting over the Laurentide ice sheet is shown, as well as strong winds in the channel between the Laurentide and Greenland ice sheets and intensive southern hemisphere westerlies. A possible glacial decrease of the Pacific trades, as simulated by the T21 model, could not be identified in the GFDL run because the modern wind field has not been presented.

The GFDL precipitation response for the northern hemisphere summer season [*Manabe and Broccoli*, 1985*b*] is presented for the sector 30°–90°N. As in the T21 simulation a general precipitation decrease is visible over the ice sheets

as well as a precipitation increase downstream of the Laurentide ice sheet over the North Atlantic.

5.2. *Goddard Institute for Space Studies Model*

Rind [1987] used the model II from the Goddard Institute for Space Studies (GISS) with prescribed SST from *CLIMAP Project Members* [1981]. The horizontal resolution of 8° in latitude and 10° in longitude is somewhat coarser than in the T21 model. The vertical coordinate in the GISS model is resolved by nine levels. The GISS model is comparable to the T21 model with regard to model physics except for two improvements in the soil part. The GISS model uses the no-flux condition for the lower boundary and includes prescribed vegetation. The GISS ice age experiment was performed in the annual cycle. For comparison with the T21 results, annual means were calculated by averaging the January and July means given by *Rind* [1987]. The annual mean and globally averaged surface air temperature and precipitation decreased in the GISS experiment by 3.5°C and 0.1 mm/d, respectively. This, compared to the T21 result of 4.7°C cooling, weaker temperature decrease is visible also in the zonal mean temperature. The T21 model decreased the temperature more strongly at the poles. At the north pole the GISS model simulates a cooling by 6°C compared to 12°C in the T21 model. At the south pole a cooling of 2°C in the GISS experiment has to be compared to a temperature decrease of 14°C in the T21 run. The tropical cooling of 1°–2°C in the zonal average was of the same order of magnitude in both models. The global structure of the temperature anomaly fields is roughly the same in the GISS and the T21 models with the exception of some regional features. In agreement with geological evidence the GISS results show a glacial warming in Alaska, which is missing in the T21 simulation. However, the glacial warming in East Antarctica, simulated by the GISS model, seems to contradict the ice core data.

The model response of the glacial wind field was comparable in both models, but the intensification of the northwesterlies between the Laurentide and the Greenland ice sheets, as modeled by the T21 model, is not visible in the GISS model, possibly due to a coarser resolution. Comparable to the T21 model, the GISS model simulates a glacial reduction of the Pacific trades in the northern hemisphere winter season.

The global patterns of precipitation anomalies also appear quite similar in both models. A regional difference occurs in the tropical rain forests where the precipitation seems to be increased in the GISS model.

5.3. *Community Climate Model*

Kutzbach and Guetter [1986] used the Community Climate Model (CCM) of the National Center for Atmospheric Research (NCAR). As in the GFDL model, the spectral domain is truncated rhombically at wave number 15, and the vertical is resolved by 9-sigma levels. The CCM is comparable to the T21 model with respect to the horizontal resolution and to model physics. The simulations of the last glacial maximum were performed for perpetual January and July conditions. The January and July results of the CCM are averaged for comparison with the T21 model ice age simulation. The globally averaged glacial reductions in the surface temperature are 3.8°C (4.7°C) for all points, 3.8°C (7.0°C) for land points, and 3.6°C (2.9°C) for ocean points (corresponding T21 values are given in parentheses). The difference between land and ocean temperature reduction, annually and globally averaged, simulated by the CCM is considerably smaller than in the T21 run. The simulated stronger glacial cooling in the T21 AGCM compared to the CCM (and GISS model) is probably related to differences in the models themselves (e.g., treatment of sea ice) and to different specification of the boundary conditions (e.g., absolute values or anomalies for the SST, maximum or minimum ice sheet elevations as given by *CLIMAP Project Members* [1981]). The response in the global fields of near-surface temperature (also wind and precipitation) is comparable in the CCM and the T21 model, except for some regional features. The CCM simulates a glacial warming in East Antarctica which contradicts the ice core data, while the relatively mild glacial climate in Alaska seems to be realistically simulated. The temperature decrease over the Tibetan Plateau is stronger in the T21 model because of the assumed additional ice sheet with a maximum elevation of 1.5 km.

The major differences of the near-surface circulation between the CCM and the T21 model are located in the tropics and in the southern hemisphere. The CCM does not seem to simulate (anomalies are not presented) a glacial decrease of the Pacific trades and a glacial intensification of the southern hemisphere westerlies. In the higher atmosphere both the CCM and T21 models simulate a glacial splitting of the jet stream over the Laurentide ice sheet.

The CCM values for the globally averaged annual mean precipitation anomalies are −0.22 mm/d (−0.26 mm/d) on land and −0.23 mm/d (+0.11 mm/d) above the ocean (corresponding T21 values are in parentheses). Again, the CCM does not simulate pronounced differences between land and ocean points. The different oceanic response in the precipitation is probably related to the different land-ocean temperature contrasts in both simulations. The air which is advected from the land to the ocean will be colder in the T21 model compared to the CCM. Thus assuming comparable evaporation in both models, oceanic precipitation will be larger in the T21 experiment. The global distributions of precipitation anomalies appear quite similar in both models, with the exception of some regional features. The precipitation in tropical rain forest areas seems to be increased in the CCM simulation.

5.4. *Rand Corporation Model*

To simulate the last glacial maximum, *Gates* [1976] used an AGCM developed at the Rand Corporation (RC). The RC model is a grid point model restricted to the troposphere (upper boundary 200 hPa). The vertical is resolved by 2-sigma levels. The horizontal resolution is 4° in latitude and 5° in longitude. The model physics, however, based on the primitive equations, is comparable to the other AGCMs. The glacial boundary conditions were specified according to *CLIMAP Project Members* [1976]. The ice age simulation with the RC model was restricted to perpetual July conditions. Nevertheless, we included the RC results in this section of model comparisons, although July anomalies are not directly comparable with annual mean anomalies. The global reduction of the surface air temperature of 4.9°C in the RC simulation is comparable to 4.7°C in the T21 ice age run. In East Antarctica, a critical region for some of the other models, the surface temperature decreases by the same amount as in the T21 model. At tropical

land surfaces the temperatures seem to decrease more strongly than in the T21 model.

The globally averaged glacial precipitation is reduced by 0.61 mm/d (14%) in the RC model, while the T21 model reduced precipitation by 0.05 mm/d (2%). In the tropical land areas the precipitation seems to be slightly increased. Contrary to geological data the Indian summer monsoon increases in the RC model.

6. Conclusions

With the exception of some regional features the simulated response of the T21 model atmosphere to ice age boundary conditions is roughly in agreement with paleogeological observations and is consistent with the results of other AGCMs. This suggests that currently available AGCMs and now also the T21 AGCM are able to simulate climatic states under boundary conditions far away from the present, although they were calibrated using present-day observations. It was shown that the mean climatic state of the atmosphere changed significantly under ice age conditions, while the basic structure of the atmospheric circulation was not altered dramatically. Some regional features of the atmospheric response to ice age conditions, however, differ for the various models and are partly in conflict with observations, especially on land. The validation of regional model response, for example, in the tropics, requires more work in the future. In the T21 model, inconsistencies at land points may arise due to the specification of the deep soil temperature and moisture at the lower boundary instead of a no-flux boundary condition.

Acknowledgments. The authors thank all three referees and T. J. Crowley (ARC Technologies, Texas) for suggestions to strengthen the analysis and the discussion of the results. The support of the Climatic Research Group of K. Hasselmann (Max-Planck-Institut für Meteorologie, Hamburg) and the General Circulation Group of G. Fischer (Universität Hamburg) in setting up and performing the presented AGCM experiments is gratefully acknowledged. We also thank B. D. Santer for carrying out the statistical analysis (only parts of which are presented in this contribution). We are grateful to M. Esch, K. Fieg, and S. Lorenz for assistance in producing the figures. The hand-drawn figures were carefully produced by M. Grunert. This project was supported by the Bundesministerium für Forschung und Technologie.

References

Atkinson, B. W., *Meso-scale Atmospheric Circulations*, Academic, San Diego, Calif., 1981.

Barnola, J. M., D. Raymond, Y. S. Korotkevich, and C. Lorius, Vostok ice core provides 160,000-year record of atmospheric CO_2, *Nature*, *329*, 408–414, 1987.

Berger, A. L., Long-term variations of daily insolation and Quaternary climatic changes, *J. Atmos. Sci.*, *35*, 2362–2367, 1978.

Broccoli, A. J., and S. Manabe, The influence of continental ice, atmospheric CO_2, and land albedo on the climate of the last glacial maximum, *Clim. Dyn.*, *1*, 87–99, 1987.

CLIMAP Project Members, The surface of the ice-age Earth, *Science*, *191*, 1131–1137, 1976.

CLIMAP Project Members, Seasonal reconstruction of the Earth's surface at the last glacial maximum, *Geol. Soc. Am., Map Chart. Ser., MC-36*, 1981.

Crowley, T. J., Paleoclimate modelling, in *Physically-Based Modelling and Simulation of Climate and Climatic Change*, Part II, edited by M. E. Schlesinger, pp. 883–949, Kluwer Academic, Boston, Mass., 1988.

Crowley, T. J., and G. R. North, *Paleoclimatology*, 414 pp., Oxford University Press, New York, in press, 1990.

Dümenil, L., and U. Schlese, Description of the general circulation model, in Climate Simulations With the T21-model in Hamburg, Large Scale Atmospheric Model, edited by G. Fischer, *Rep. 1*, pp. 3–9, Meteorol. Inst., Univ. of Hamburg, Germany, 1987.

Duplessy, J. C., Glacial to interglacial contrasts in the northern Indian Ocean, *Nature*, *295*, 494–498, 1982.

Gates, W. L., The numerical simulation of ice-age climate with a global general circulation model, *J. Atmos. Sci.*, *33*, 1844–1873, 1976.

Jaeger, L., Monatskarten des Niederschlags für die ganze Erde, *Ber. Dtsch. Wetterdienstes*, *18*(139), 38, 1976.

Jouzel, J., C. Lorius, J. R. Petit, C. Genthon, N. I. Barkov, V. M. Kotlyakov, and V. M. Petrov, Vostok ice core: A continuous isotope temperature record over the last climatic cycle (160,000 years), *Nature*, *329*, 403–408, 1987.

Kuhle, M., Subtropical mountain- and highland glaciation as ice age triggers and the waning of the glacial periods in the Pleistocene, *GeoJournal*, *14*, 393–421, 1987.

Kutzbach, J. E., and P. J. Guetter, The influence of changing orbital parameters and surface boundary conditions on climate simulations for the past 18,000 years, *J. Atmos. Sci.*, *43*, 1726–1759, 1986.

Lautenschlager, M., and B. D. Santer, Atmospheric response to a hypothetical Tibetan ice-sheet, *J. Clim.*, in press, 1990.

Liu, K., and P. A. Colinvaux, Forest changes in the Amazon basin during the last glacial maximum, *Nature*, *318*, 556–557, 1985.

Louis, J.-F., ECMWF forecast model: Physical parameterization, *Res. Manual 3*, Eur. Cent. for Medium-Range Weather Forecasts, Res. Dep., Reading, England, 1984.

Manabe, S., and A. J. Broccoli, A comparison of climate model sensitivity with data from the last glacial maximum, *J. Atmos. Sci.*, *42*, 2643–2651, 1985*a*.

Manabe, S., and A. J. Broccoli, The influence of continental ice sheets on the climate of an ice age, *J. Geophys. Res.*, *90*, 2167–2190, 1985*b*.

Messerli, B., Die afrikanischen Hochgebirge und die Klimageschichte Afrikas in den letzten 20,000 Jahren, in *Das Klima—Analysen und Modelle, Geschichte, und Zukunft*, edited by H. Oeschger, B. Messerli, and M. Svilar, pp. 64–90, Springer-Verlag, New York, 1980.

Petit, J.-R., M. Briat, and A. Royer, Ice age aerosol content from East Antarctic ice core samples and past wind strength, *Nature*, *293*, 391–394, 1981.

Pisias, N. G., and D. K. Rea, Late Pleistocene paleoclimatology of the central equatorial Pacific: Sea surface response to the southeast trade winds, *Paleoceanography*, *3*, 21–37, 1988.

Rind, D., Components of the ice age circulation, *J. Geophys. Res.*, *92*, 4241–4281, 1987.

Rind, D., and D. Peteet, Terrestrial conditions at the last glacial maximum and CLIMAP sea-surface temperature estimates: Are they consistent?, *Quat. Res.*, *24*, 1–22, 1985.

Santer, B. D., and T. M. L. Wigley, Regional validation of means, variances, and spatial patterns in general circulation model control runs, *J. Geophys. Res.*, *95*, 829–850, 1990.

Sarnthein, M., K. Winn, J.-C. Duplessy, and M. R. Fontugue, Global variations of surface ocean productivity in low and mid-latitudes: Influence on CO_2 reservoirs of the deep ocean and atmosphere during the last 21,000 years, *Paleoceanography*, *3*, 361–399, 1988.

Street-Perrott, F. A., and S. A. Harrison, Temporal variations in lake levels since 30,000 yr BP—An index of the global hydrological cycle, in *Climate Processes and Climate Sensitivity*, *Geophys. Monogr. Ser.*, vol. 29, edited by J. E. Hansen and T. Takahashi, pp. 118–129, AGU, Washington, D. C., 1984.

Wigley, T. M. L., and B. D. Santer, Statistical comparison of spatial fields in model validation, perturbation, and predictability experiments, *J. Geophys. Res.*, *95*, 851–865, 1990.

K. Herterich and M. Lautenschlager, Max-Planck-Institut für Meteorologie, Bundesstrasse 55, D-2000, Hamburg 13, Federal Republic of Germany.

(Received October 12, 1989;
revised April 30, 1990;
accepted August 20, 1990.)